

NANOPARTICLE BED DEPOSITION BY SLOT DIE COATING FOR MICROSCALE SELECTIVE LASER SINTERING APPLICATIONS

Dipankar Behera*, Nilabh K. Roy*, Chee S. Foong†, and Michael Cullinan*

*Department of Mechanical Engineering, The University of Texas at Austin, Austin, TX

†NXP Semiconductors, Austin, TX

Abstract

The minimum feature size in most commercially available metal additive manufacturing (AM) processes is limited to ~100 microns which poses a fundamental challenge in fabricating complex 3D micro-components. The authors have developed a microscale selective laser sintering (μ -SLS) process with the goal of fabricating these microproducts with 1 μ m minimum feature size resolution. To achieve near-net shaped sintered features, the powder bed layer should not be more than one micron thick. This paper presents the development and testing of a powder bed deposition mechanism using a slot-die coater. Metallic nanoparticles uniformly dispersed in a solvent were used in this study. A viscocapillary coating model was used to predict the wet thickness of the powder bed based on the coating gap. Experimental results revealed that uniform sub-micron layer thicknesses were achieved by optimizing the process parameters such as flow rate, coating speed, coating gap, and die gap. The novel approach discussed in this paper enables the implementation of a robust coating mechanism for high throughput AM.

Introduction

AM has traditionally driven the development of high throughput techniques for the fabrication of complex and specialized three-dimensional products. Recent innovations in these technologies are being targeted at integrating the manufacture of true-3D architectures with other processes. While these processes are well designed for macroscale and mesoscale part fabrication, there are several challenges involved in downscaling them to micron and sub-micron sizes. Although microfabrication of polymer structures using stereolithography (SL) has been commercialized extensively, most microscale AM processes for metals are still in prototyping phases. Typical metal AM processes are based on powder bed fusion (SLS, LM) and are limited to a minimum layer thickness of 50 μ m. Limited laser focus, uneven agglomeration of finer particles and higher susceptibility to oxidation, largely undermine the fidelity of the metal AM processes [1], [2]. Addressing these challenges, the authors have developed the μ -SLS process for fabrication of true-3D sintered metal structures with a 1 micron target resolution [3].

A target application of the μ -SLS process is to fabricate interconnects for Integrated Circuits (ICs). An ever-increasing demand for the miniaturization of electronic components has spurred the need for the development of 3D multichip modules. Their performances are affected by interconnects like C4 solder bumps, vias, BGAs, and conducting pads etc. within and between the chip components. A SL based 3D electronic structure was reported by Lopes *et al* [4]. Cai *et al* [5] presented 10 μ m high microstrip lines and vertical interconnects with 20 μ m planar resolution using the Aerosol Jet Printing (AJP) process. However, the resolution of many extrusion and

printing techniques are inherently limited by the diameter of their nozzles, as smaller nozzles require higher operating pressures to avoid clogging of the nozzles. While Electrohydrodynamic (EHD) printing can address this problem by applying a potential difference across the conductive nozzle and the ink to achieve sub-micron droplets, the effect of highly charged droplets on the final part resolution is still an active area of interest [6].

This paper explores the deposition of conductive ink in a layer-by-layer fashion via a coating method. The coating process for μ -SLS should be able to dispense uniform sub-micron layers of low viscosity nanoparticle inks (NP inks) to achieve near net shape features. Another desirable feature in the system would be its compatibility with different substrates, including flexible substrates and roll-to-roll flexibility so that it can be employed in the upcoming versions of the μ -SLS system. A simplified process flow of the μ -SLS system has been shown in figure 1. A slot die coating method is used to obtain sub-micron layer thicknesses for deposition of metallic nanoparticle inks. While a variety of coating techniques are available (spin coating, curtain coating, spray coating etc.), the slot die coating method offers higher scalability and lower material wastage. It can achieve a coating thickness ranging from tens of nanometers to hundreds of microns. The design of a slot die coater can be optimized to include a wide range of liquids.

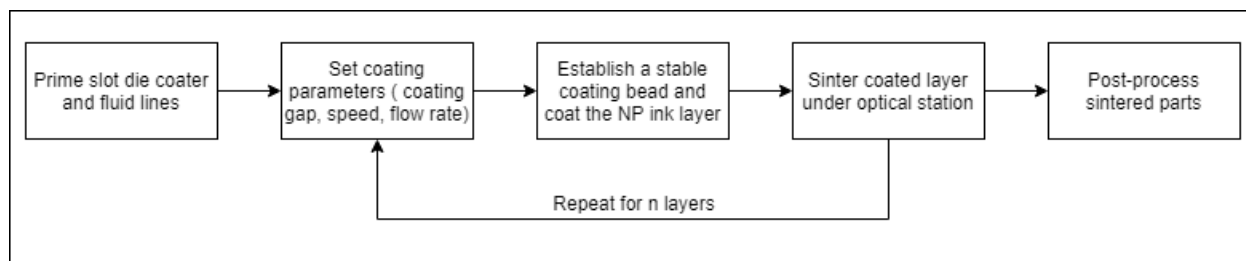


Figure 1: Simplified process flow schematic of the μ -SLS system.

To achieve submicron layer thicknesses, the particle size must be smaller than that. Roy et al [7] investigated the effect of particle size and morphology on the sintering quality. Copper (Cu) NPs were used because of their excellent electrical properties and lower costs, compared to gold (Au) and silver (Ag). Dry Cu nanopowders exhibited uncontrolled agglomeration which was attributed to high van der Waals' forces between the particles to minimize the surface energy of the powder bed. In addition, precisely spreading them to achieve a high packing density is very difficult. Therefore, Cu and Ag nanoparticle inks were tested which demonstrated significantly lower agglomeration. These inks were chosen as the preferred method of particle bed deposition for the sintering process.

Slot Die Coating Background

The slot die coating process was invented by Beguin to coat gelatin Silver Halide layers for making photographic films [8]. The process can be used with a variety of organic and inorganic liquids and it can accommodate a wide range of fluid viscosities. The slot die coating process is the preferred manufacturing method for lithium-ion batteries, polymer electrolytic membrane fuel cells (PEMFCs), flat panel and flexible electronics, and solar batteries [9]–[11]. The versatility of this process allows us to use a variety of nanoparticle inks from different manufacturers and

understand the coating process better. The liquid enters a fixed slot inside a precisely machined die and establishes contact with a moving substrate. It is a pre-metered coating process where the thickness of the coated layer is a function of the flow rate of the liquid and the substrate speed. After the gap between the die lips and the substrate, also known as the coating gap, is filled with liquid, the coating bead is established. The stability of the coating bead determines the quality of coating. Coating uniformity is dependent on other process parameters like the flow rate, coating speed, vacuum pressure, die geometry, and rheological properties of the liquid [12].

Conventional applications of the slot die coating system exhibit large area uniformity of continuous layers in roll-to-roll systems. The continuity of the process, along with the identification of the operability window, ensures the stability of the coating bead, thereby reducing coating related defects like ribbing, rivulets, and air entrapment. The current design of the μ -SLS system, however, makes this a non-continuous, intermittent and layer-by-layer process. Intermittent coating reduces the process throughput and leads to higher levels of material wastage during the start-up and end of the slot die coating process. There has not been significant research on intermittent coating of multiple layers. This introduces additional challenges in defining the coating parameters for high quality coating. Also, understanding the results of layer-by-layer coating is another area of research experimentally explored in this study. Therefore, in this study, we have attempted to experimentally optimize the coating parameters to achieve sub-micron layers of metal NP inks.

Slot Die Coater Design

The experimental setup is shown in figure 2. The major sub-components of the slot die system include the positioning mechanism, syringe pump, and the die assembly. The slot die coater is designed and manufactured by nTact [13]. The positioning mechanism translates the die head vertically for subsequent layer depositions. It is a precision ball screw linear rail with 3-micron positioning repeatability and backlash, driven by a 0.36 degree microstepping motor. The microstepping motor is controlled by a TinyG controller [14] which provides precise multi-axis motor control. A cylindrical flexural pivot with a micrometer is used for in-plane positioning of the die head. A 60mm stroke Kloehn/IMI Norgren V6 series syringe pump with a three-way rotary valve assembly is used as the metallic nanoparticle ink input source to the slot die coater. A zero dead volume tip UHMW syringe, driven by a precision ball screw, ensured that no fluid remained, and all air bubbles were removed from the system. The valve is operated by a NEMA 23 stepper motor to alternate the distribution and aspiration functions.

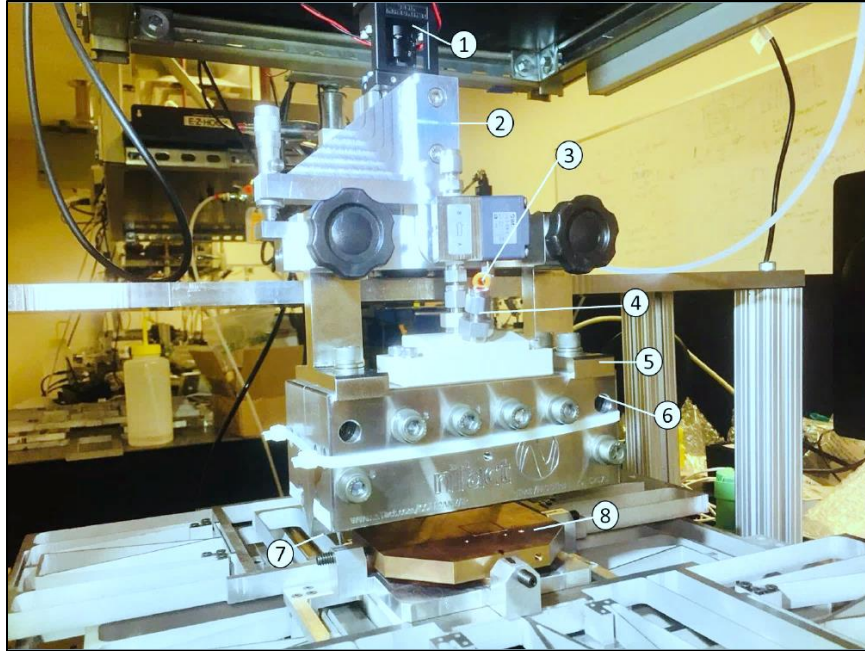


Figure 2: Components in the assembly of the slot die coating system- 1. z-direction motor coupled with 100mm travel leadscrew 2. Pivoting bracket 3. Input for air pilot valve 4. Slot die input 5. Die support Arms 6. Die head 7. Die lips 8. Substrate

However, it is very difficult to achieve $<10\ \mu\text{m}$ film thickness without having accurate control over the coating gap, due to inherent assembly and machining tolerances. The primary approach is to facilitate multiple layer coating capability without distorting the layers underneath. This also introduced additional challenges at the design stage. The slot die lips needed to be parallel to the substrate within a specified tolerance corresponding to the datum points. These errors affect the parallelism between the substrate and the die lips, which can lead to machine crashes. Currently, the parallelism is checked manually using precision shims, however a more robust method using capacitance probes is being developed by the authors to measure the coating gap at three different points as the die is vertically translated.

Viscocapillary Model

The liquid layer between the substrate and the die lips is bound by an upper and lower meniscus. The upstream meniscus initiates the formation of the coating bead and the downstream meniscus facilitates the spreading of the liquid on the moving die. The range of operating parameters, i.e. the coating gap, die gap, substrate speed, and upstream vacuum pressure, etc. is defined by a coating window [15]. While an analytical method can be used to determine these parameters for multilayer coatings, the high experimentation costs make it imperative to understand the theoretical models to set the initial coating parameters. While modeling a single layer coating process, one of the critical parameters which needs to be monitored is the coating gap to film thickness ratio. The flow between the die and the substrate is governed by a combination of different forces, primarily viscous, capillary, and inertial forces [12]. The coating bead is defined as being stable when the coated layer is uniform and free of defects like air entrainment, ribbing, and rivulets etc. The stability of the coating bead is determined by the

operating limits of the process parameters. The minimum wet film thickness corresponding to a given coating speed is known as the low-flow limit. The coating bead becomes unstable and breaks if the coating speed is outside the low-flow limit.

Ruschak [16] developed a one-dimensional capillary model based on an extension of the Landau-Levich law which determined the minimum coating thickness of a film dragged by a plate. The primary assumption of Ruschak's model is that the viscous effects are negligible. However, the Landau-Levich boundary conditions assume that the coating speed and flow rate of the liquid approach zero. This renders the model valid for low capillary number and low Reynolds number liquids. The operating limits defined by Ruschak's model showed that the minimum wet film thickness is directly proportional to the coating gap and speed, and established a range of pressure drop across the downstream meniscus of the die, as shown in equations 1 and 2, respectively. Here, t is the thickness of the wet film, h_d is the downstream coating gap and Δp is the pressure difference across the coating bead. Ca is the capillary number, defined as the ratio of viscous forces to interfacial forces, $\frac{\mu V}{\sigma}$, where μ is the dynamic viscosity of the liquid, V is the coating speed and σ is the surface tension.

$$t \geq 0.67h_dCa^{2/3} \quad (1)$$

$$\frac{\sigma_u(1-\cos\theta)}{h_u} + 1.34Ca^{2/3}\frac{\sigma_d}{t} \leq \Delta p \leq \frac{\sigma_u(1-\cos\theta)}{h_u} + 1.34Ca^{2/3}\frac{\sigma_d}{t} \quad (2)$$

Since the capillary number for the nanoparticle ink used in this study varies from 0.001 to 0.02, Ruschak's model can be used to characterize the coating speed and coating gap required for a required wet film thickness. Figure 3 shows the relationship between minimum wet film thickness and the capillary number, which increases with the coating speed. The rectangular window represents the range of coating speeds and gaps which can be used during the experiments to coat a film of specific thickness. The film thickness is also directly proportional to the coating gap. The input flow rate into the die was increased to sustain the coating bead stability at higher speeds. A 1-micron wet film thickness is required for the resolution requirement of the μ -SLS process. This model was used to identify a low-flow limit window which provided the authors with the coating speed and coating gap values for a given wet film thickness.

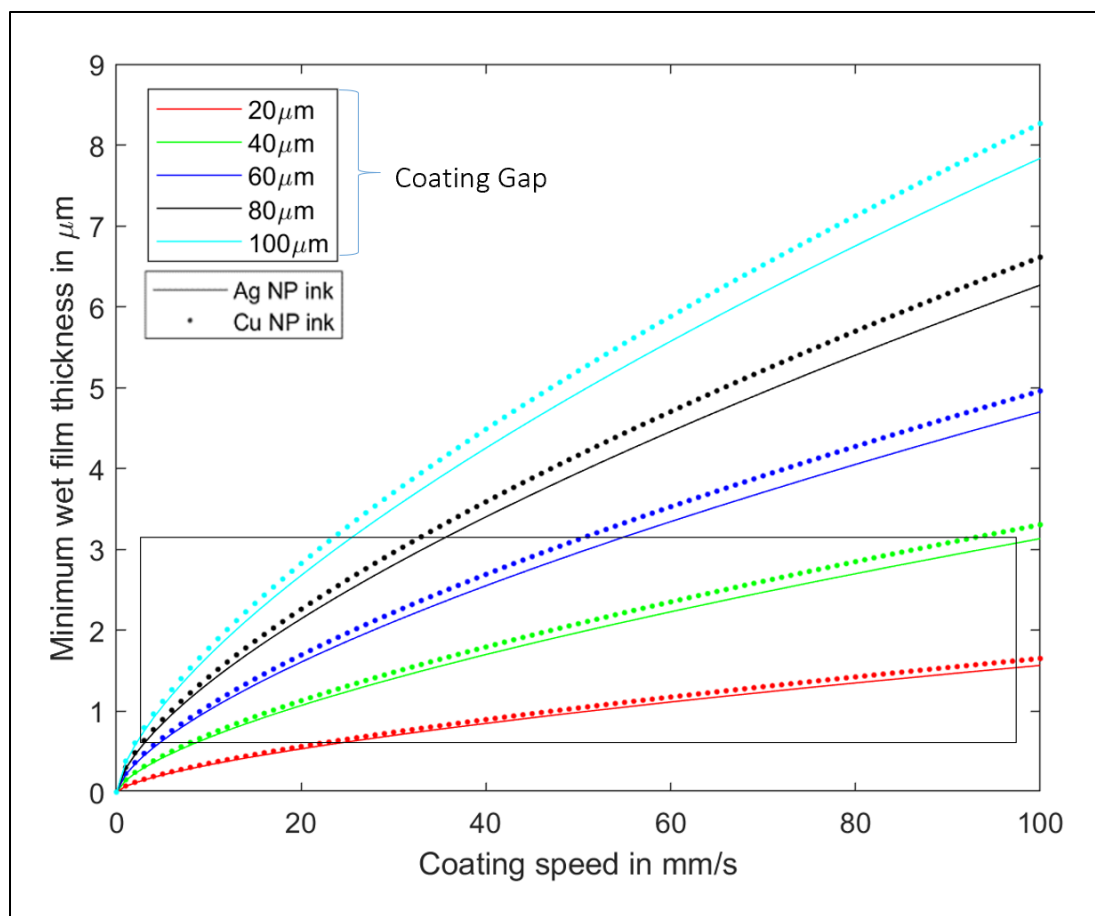


Figure 3: Minimum wet film thickness (in μm) versus coating speed (in mm/s).

Results and Discussions

During the start-up of the slot die coating process, initial priming of the NP ink into the fluid lines and the die gap is required. The upstream die is currently under ambient pressure, as a vacuum chamber is not being used. The die gap is set using a $50\ \mu\text{m}$ thin Polyether ether ketone (PEEK) shim. The coating gap is measured using a Keyence IL030 laser triangulation sensor [17] to the die head and the measurement of its displacement by the vertical positioner. However, it is difficult to accurately define the planarity of the die head with respect to the substrate. A rigid mount is being developed by the authors which holds three capacitive sensors for planar tip-tilt correction. The substrate is moved via a long-range translation stage supported by two air bearing platforms. Once the slot die coater lines are primed and purged of air bubbles, the initial coating bead is established. As the substrate starts moving at the specified coating speed, the flow rate of the liquid entering the die is varied to maintain the stability of the bead. The coated substrate is completely dried at $85\text{-}90^\circ\text{C}$ for 15-25 minutes depending on the wet layer thickness and type of NP ink used.

The dried Cu NP ink thickness is measured using an optical profilometer. The coating thickness is higher during the establishment of the coating bead. This led to an overflow of excess ink along the direction of coating, and therefore limited the uniformity of coating. A possible

solution to intermittent slot die coating is to initially establish the coating bead outside the sample area and then re-initiate the flow once the liquid flow inside the die has reached steady state. Figure 4a shows the average dried film thicknesses achieved for varying coating gaps. The flow rate into the die is varied from 2.5mL/min to 5 mL/min. The coating speed is adjusted based on the coating gap to avoid low flow limits. The samples with coating gaps of 50 μm and 75 μm were coated at 10 mm/s and samples with 100 μm and 125 μm are coated at 15 mm/s. The thickness data is measured at multiple points along the direction of coating and across the samples. A measurement plot showing the dried film thickness uniformity for a 75 μm coating gap is shown in figure 4b. Higher speeds at lower flow rates would often introduce coating defects like loss of coating bead, which is expected as per the coating models.

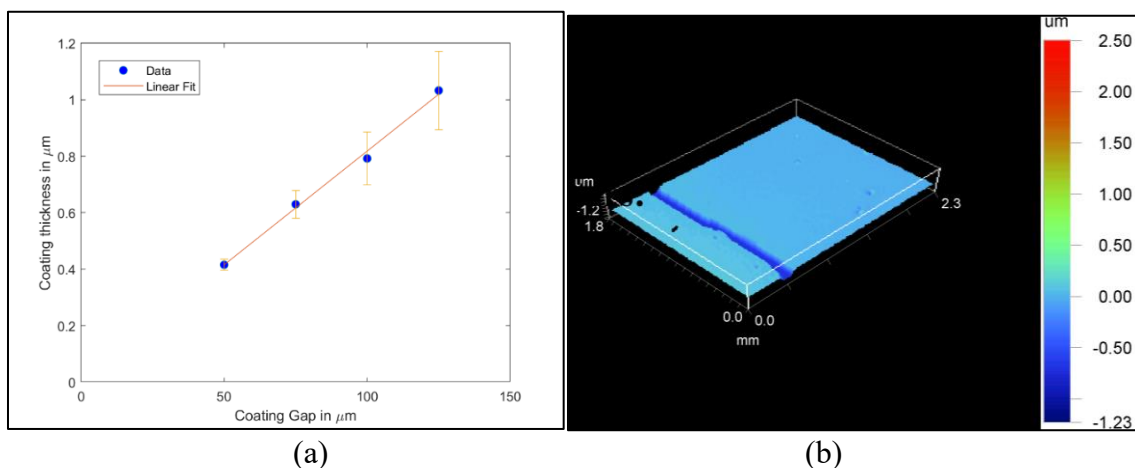


Figure 4. a) Experimental dry film thickness (in μm) versus coating gap (in μm) b) Optical profilometry 3D plot showing the coating uniformity

An important consideration for the μ -SLS system is that the nanoparticle bed is uniformly distributed and devoid of any agglomeration. The SEM images figure 5 compares the particle distribution of nanopowders, spin-coated Cu NP ink and slot-die coated Cu and Ag NP ink. As can be observed from the images, the agglomeration in slot die coated samples is lower compared to the spin coated samples. The spreading uniformity were also more consistent in the slot die coated samples.

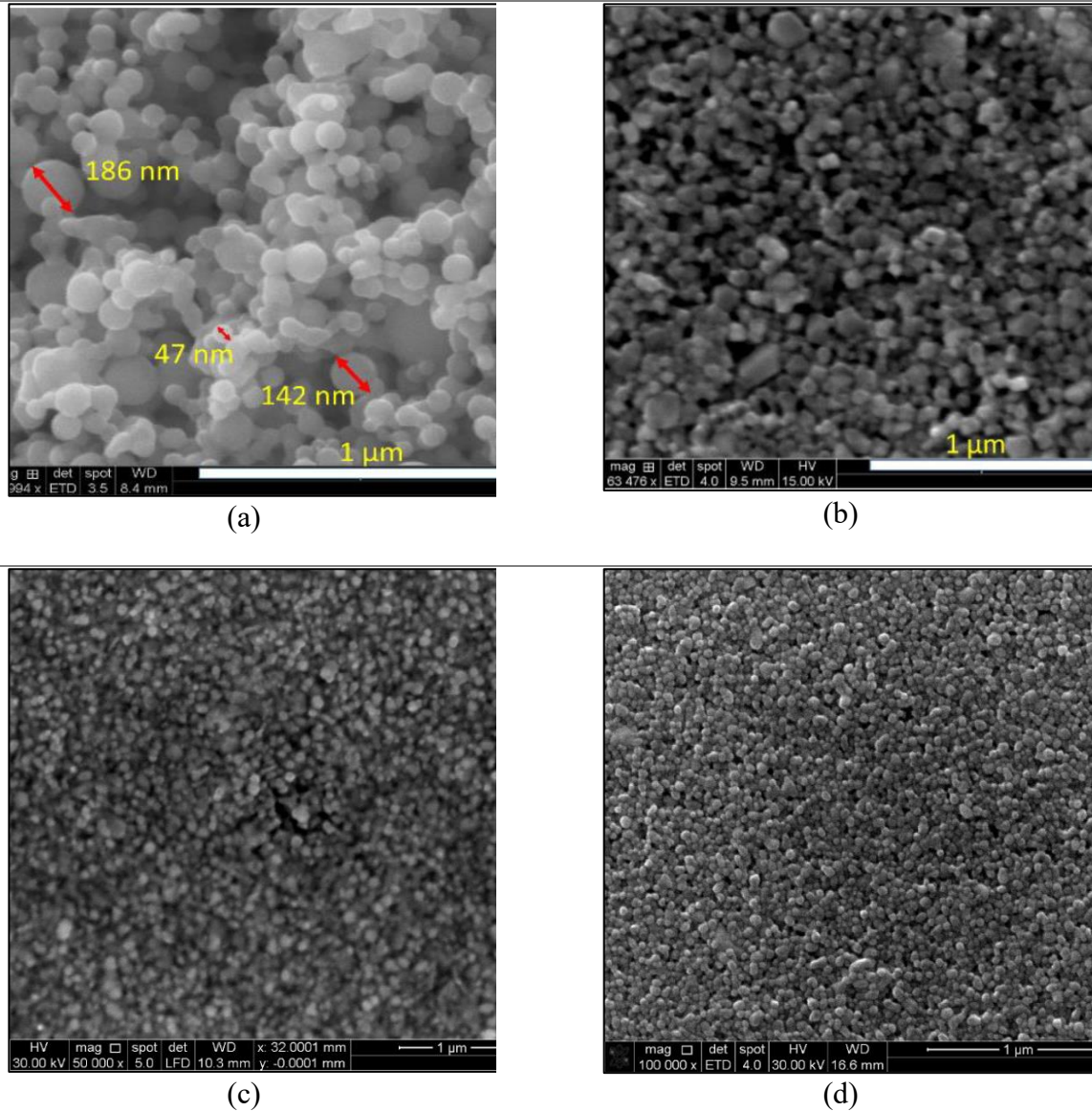


Figure 5. Scanning electron micrographs for: a) Cu nanopowders, b) Spin coated Cu NP ink sample, c) Slot die coated Cu NP ink, d) Slot die coated Ag NP ink.

After the first layer was coated, the coating gap was fixed at 100 μm and a subsequent layer was laid on top of the previous one. The preliminary results show that the dried film thickness in the ideal coating region of the two-layer film is 1.73 times that of the single layer thickness. A 50W, 808 nm continuous wave (CW) laser was used to sinter nanoparticle inks for the μ -SLS process. A Digital Micromirror Device (DMD) [18] is used to project the pattern on the ink bed using a set of primary optics inside the DMD assembly. Secondary focusing optics are used to adjust the focal plane of the projected image. Initial sintering experiments showed that the energy lost before reaching the substrate was $\sim 90\%$ due to lossy primary and secondary optics inside, hence sufficient sintering of Cu NP ink was not achieved. The maximum irradiance at sample plane is 500 W/cm^2 , which is much smaller than sintering Cu NP ink at 50 ms with the current optical system. Therefore, Ag NP ink was used for the sintering experiments, as the irradiance

requirement was within the bounds of the current optical setup, given that the sintering exposure durations are high. For the initial sintering experiment, a 500 μm circle was sintered. The first layer of the coated substrate (100 μm coating gap) was partially dried to remove excess solvent at 85 $^{\circ}\text{C}$ for 5-7 minutes and then sintered at 50W, 4 seconds exposure duration. The average height of the sintered circle was 2.37 μm . Another sample was coated and sintered at the same parameters. The sintered sample was coated again at a 100 μm coating gap and then dried. After the second layer was dispensed on the top of the first layer, the same circular pattern was sintered at an exposure duration of 6 seconds. The average height of the 2 layers was around 5.54 μm . Excess NP ink was removed from both the samples by ultrasonically treating them. Figure 6a and b show the 3D profilometer images of the sintered circles for layer 1 and layer 2 respectively. Figure 6c and d show sample average heights of sintered circles for layer 1 and layer 2 respectively. The bilayer sintered sample is 2.34 times higher than the single layer sample. During post processing measurements, it was noticed that the heat affected zones in the multilayer sample were larger than the single layer sample.

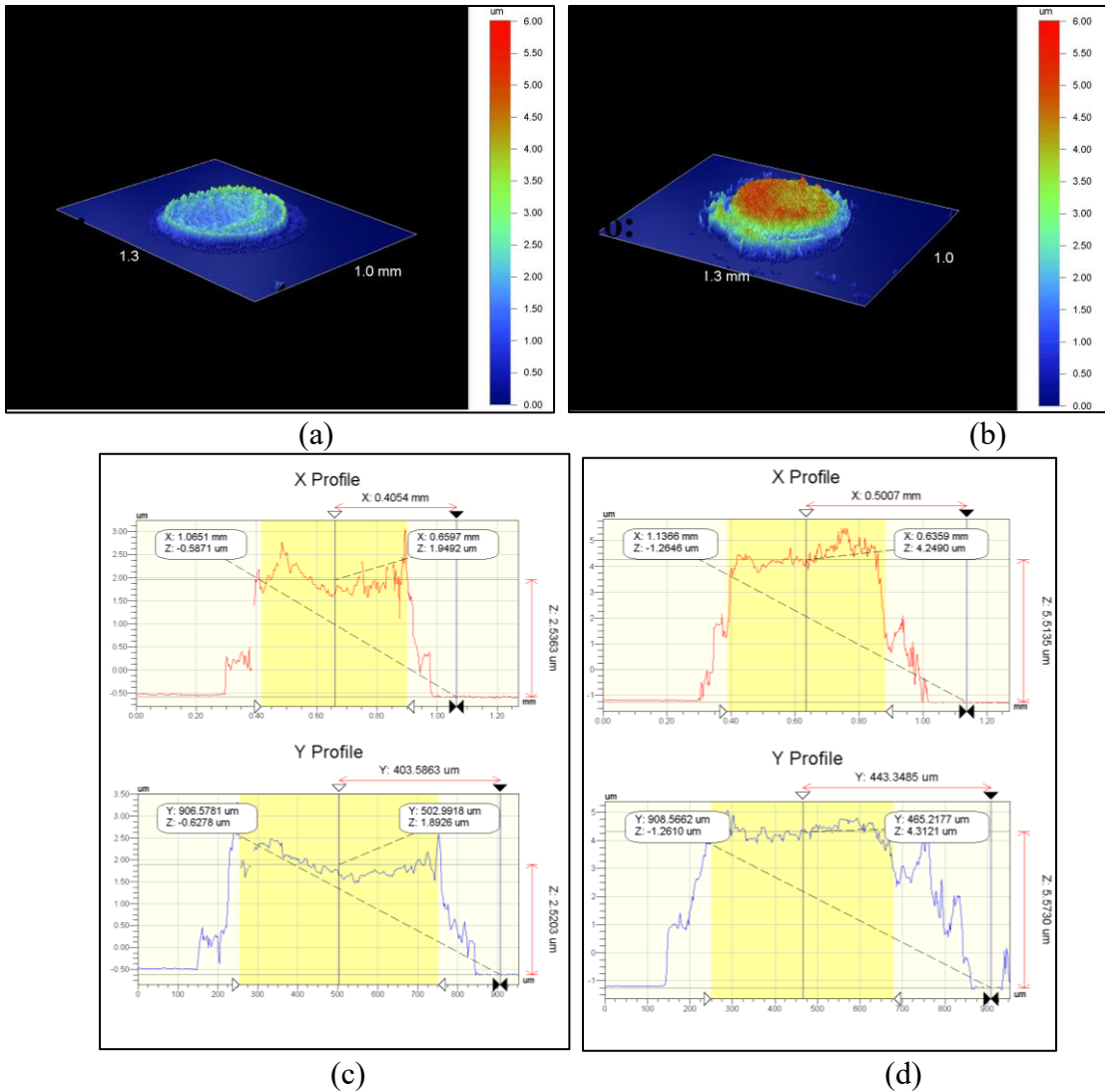


Figure 6. 3D profile of a) single layer sintered sample, b) bilayer sintered sample.

2D profile measurements along diameter for c) single layer sintered sample, d) bilayer sintered sample

Conclusions and Future Work

A novel nanoparticle layer dispense technique, using the slot die coating method for a microscale selective laser sintering process has been discussed. The critical slot die coating parameters like coating speed and flow rate are investigated, and the dry film thickness is measured. The dry film thickness was increased linearly with the coating gap. Preliminary sintering experiments show that the sintered part height of a two-layer coating was 2.34 times the single layer coating. To progress with the design development of the multilayer slot die system and optimization of the associated process parameters, a comprehensive study of an extensive series of film thicknesses will be completed. This would enable the authors to characterize the non-linearity of the coating film thicknesses in layer-by-layer coating. Another critical parameter to investigate will be the effect of drying conditions on the coating and sintering quality. This research has shown that the slot die subsystem of the μ -SLS tool can coat submicron nanoparticle ink layers.

References

- [1] M. Vaezi, H. Seitz, and S. Yang, "A review on 3D micro-additive manufacturing technologies," *Int. J. Adv. Manuf. Technol.*, vol. 67, no. 5–8, pp. 1721–1754, 2013.
- [2] L. Hirt, A. Reiser, R. Spolenak, and T. Zambelli, "Additive Manufacturing of Metal Structures at the Micrometer Scale," *Adv. Mater.*, vol. 29, no. 17, 2017.
- [3] N. Roy, A. Yuksel, and M. Cullinan, "Design and Modeling of a Microscale Selective Laser Sintering System," *Proc. 27th Solid Free. Fabr. Symp.*, p. V003T08A002-V003T08A002, 2016.
- [4] A. J. Lopes, E. MacDonald, and R. B. Wicker, "Integrating stereolithography and direct print technologies for 3D structural electronics fabrication," *Rapid Prototyp. J.*, vol. 18, no. 2, pp. 129–143, 2012.
- [5] F. Cai *et al.*, "Low-Loss 3-D Multilayer Transmission Lines Manufacturing Technologies," vol. 64, no. 10, pp. 3208–3216, 2016.
- [6] K. Barton, S. Mishra, K. A. Shorter, A. Alleyne, P. Ferreira, and J. Rogers, "A desktop electrohydrodynamic jet printing system," *Mechatronics*, vol. 20, no. 5, pp. 611–616, 2010.
- [7] N. K. Roy, C. S. Foong, and M. A. Cullinan, "Effect of size, morphology, and synthesis method on the thermal and sintering properties of copper nanoparticles for use in microscale additive manufacturing processes," *Addit. Manuf.*, vol. 21, no. February, pp. 17–29, 2018.
- [8] A. E. Beguin, "June 15, 1954," US2681294A, 1954.
- [9] M. Schmitt, R. Diehm, P. Scharfer, and W. Schabel, "An experimental and analytical study on intermittent slot die coating of viscoelastic battery slurries," *J. Coatings Technol. Res.*, vol. 12, no. 5, pp. 927–938, 2015.
- [10] K. L. Bhamidipati, S. Didari, and T. A. L. Harris, "Slot die coating of polybenzimidazole based membranes at the air engulfment limit," *J. Power Sources*, vol. 239, pp. 382–392, 2013.
- [11] K. J. Choi, J. Y. Lee, J. Park, and Y. S. Seo, "Multilayer slot-die coating of large-area organic light-emitting diodes," *Org. Electron. physics, Mater. Appl.*, vol. 26, pp. 66–74, 2015.
- [12] X. Ding and J. Liu, "REVIEW ARTICLE : TRANSPORT PHENOMENA AND FLUID MECHANICS A Review of the Operating Limits in Slot Die Coating Processes," vol. 62, no. 7, 2016.
- [13] "Extrusion Deposition Systems | Extrusion Coating | nRad | nTact | nTact." [Online]. Available: <https://ntact.com/products/nrad-systems/>. [Accessed: 24-Aug-2018].
- [14] "TinyG CNC Controller - Synthetos." [Online]. Available: <https://synthetos.myshopify.com/products/tinyg>. [Accessed: 24-Aug-2018].
- [15] J. Nam and M. S. Carvalho, "Two-layer tensioned-web-over-slot die coating : Effect of operating conditions on coating window," *Chem. Eng. Sci.*, vol. 65, no. 13, pp. 4065–4079, 2010.
- [16] K. J. Ruschak, "LIMITING FLOW IN A PRE-METERED COATING DEVICE," vol. 31, 1976.
- [17] "IL-030 - Sensor heads | IL series | KEYENCE America." [Online]. Available: <https://www.keyence.com/products/measure/laser-1d/il/models/il-030/index.jsp>. [Accessed: 24-Aug-2018].

- [18] “DLP Getting Started | DLP Products | TI.com.” [Online]. Available: <http://www.ti.com/dlp-chip/getting-started.html>. [Accessed: 24-Aug-2018].